Photochemical Green Synthesis of Calcium-Alginate-Stabilized Ag and Au Nanoparticles and Their Catalytic Application to 4-Nitrophenol Reduction

ARTICLE *in* LANGMUIR · DECEMBER 2009

Impact Factor: 4.46 · DOI: 10.1021/la902950x · Source: PubMed

5 AUTHORS, INCLUDING:

Sandip Saha
National Sun Yat-sen University
21 PUBLICATIONS **497** CITATIONS
SEE PROFILE

Anjali Pal
IIT Kharagpur
141 PUBLICATIONS **4,333** CITATIONS
SEE PROFILE

Subrata Kundu
Texas A&M University
94 PUBLICATIONS **3,073** CITATIONS
SEE PROFILE

Tarasankar Pal
IIT Kharagpur
256 PUBLICATIONS **8,768** CITATIONS
SEE PROFILE

Langmuir
Article
pubs.acs.org/Langmuir

Photochemical Green Synthesis of Calcium-Alginate-Stabilized Ag and Au Nanoparticles and Their Catalytic Application to 4-Nitrophenol Reduction

Sandip Saha,[†,‡] Anjali Pal,*[,†] Subrata Kundu,[§] Soumen Basu,[‡] and Tarasankar Pal[‡]

[†]*Department of Civil Engineering and* [‡]*Department of Chemistry, Indian Institute of Technology, Kharagpur 721302, India.* [§] *Present address: Department of Materials Science and Mechanical Engineering, Texas A&M University, College Station, Texas 77843-3123*

Received August 9, 2009. Revised Manuscript Received November 6, 2009

Silver and gold nanoparticles have been grown on calcium alginate gel beads using a green photochemical approach. The gel served as both a reductant and a stabilizer. The nanoparticles were characterized using UV−visible spectroscopy, X-ray diffraction (XRD), scanning and transmission electron microscopy (SEM and TEM), energy dispersive X-ray (EDS), and selected area electron diffraction (SAED) analyses. The particles are spherical, crystalline, and the size ranges for both Ag and Au nanoparticles are < 10 nm. It is noticed from the sorption experiment that the loading of gold on calcium alginate beads is much more compared to that of Ag. The effectiveness of the as-prepared dried alginate-stabilized Ag and Au nanoparticles as a solid phase heterogeneous catalyst has been evaluated, for the first time, on the well-known 4-nitrophenol (4-NP) reduction to 4-aminophenol (4-AP) in the presence of excess borohydride. The reduction was very efficient and followed zero-order kinetics for both Ag and Au nanocomposites. The effects of borohydride, initial 4-NP concentration, and catalyst dose were evaluated. The catalyst efficiency was examined on the basis of turnover frequency (TOF) and recyclability. The catalytic efficiency of alginate-based Ag catalyst was much more compared to that of the Au catalyst. The as-prepared new solid-phase biopolymer-based catalysts are very efficient, stable, easy to prepare, eco-friendly, and cost-effective, and they have the potential for industrial applications.

Introduction

In recent years, metal nanoparticles have been investigated extensively[1−6] to understand their physical and chemical properties, not only for scientific knowledge but also for technological applications. In the nano size regime, metal nanoparticles show noticeable changes in their electrical, optical, and catalytic properties. A significant change in reduction potential is observed for metal nanoparticles of different sizes in comparison to bulk metals as the Fermi potential of nanoparticles becomes more negative. This particular property allows them to act as catalysts in various electron transfer processes.[7] In the past decade, the design of metal−polymer hybrid nanocomposite materials has attracted much attention for their wide applications in several fields from controlled devices to catalysis. Some of them have also been designed as metallic core−shell biopolymer nanocomposites for application in spectroscopy such as surface enhanced Raman scattering (SERS).[8] A few reports on biopolymer-supported metal oxides have also been published.[9,10] Application of biopolymer matrix for the synthesis of nanoparticles is important because of its potential applications in biomedical fields.[11−14] Since the inception of green chemistry approaches for sustainable development, finding out green routes for nanoparticle synthesis has remained a challenge. Furthermore, nanoparticles have been applied to easy, low-energy pathways for manufacturing industrially important products.[15] Another befitting application of nanoparticles is in environmental remediation utilizing nanoparticle-based technologies.[16,17] Thus, impregnation of nanocatalysts on renewable and nonhazardous materials (especially biomaterials) has been of immense importance in the present day context.

Manufacturing of many analgesic and antipyretic drugs, such as paracetamol, phenacetin, and so on, needs 4-aminophenol (4-AP) as a potent intermediate. It is also used enormously as a photographic developer, corrosion inhibitor, anticorrosion-lubricant, and hair-dyeing agent.[18,19] Thus, being a common precursor material for 4-AP, a newer and cheaper method for catalytic hydrogenation of 4-nitrophenol (4-NP) is always in demand. The conventional methods for hydrogenation of 4-NP involve iron/acid as a reducing agent.[20] However, use of metallic reagents has

*To whom correspondence should be addressed. E-mail: anjalipal@civil.iitkgp.ernet.in.

(1) El-Sayed, M. A. *Acc. Chem. Res.* **2004**, *37*, 326–333.
(2) Henglein, A. *J. Phys. Chem.* **1993**, *97*, 5457–5471.
(3) Murphy, C. J.; Gole, A. M.; Stone, J. W.; Sisco, P. N.; Alkilany, A. M.; Goldsmith, E. C.; Baxter, S. C. *Acc. Chem. Res.* **2008**, *41*, 1721–1730.
(4) Kamat, P. V. *J. Phys. Chem. B* **2002**, *106*, 7729–7744.
(5) Belloni, J. *Curr. Opin. Colloid Interface Sci.* **1996**, *1*, 184–196.
(6) Rosi, N. L.; Mirkin, C. A. *Chem. Rev.* **2005**, *105*, 1547–1562.
(7) Corrain, B., Schmid, G., Toshima, N., Eds. *Metal Nanoclusters in Catalysis and Materials Science The Issue of Size Control*; Elsevier: Amsterdam, The Netherlands, 2008
(8) Saha, S.; Pal, A.; Pande, S.; Sarkar, S.; Panigrahi, S.; Pal, T. *J. Phys. Chem. C* **2009**, *113*, 7553–7560.
(9) Chen, K. L.; Mylon, S. E.; Elimelech, M. *Langmuir* **2007**, *23*, 5920–5928.
(10) Gao, S.; Shi, Y.; Zhang, S.; Jiang, K.; Yang, S.; Li, Z.; Takayama-Muromachi, E. *J. Phys. Chem. C* **2008**, *112*, 10398–10401.
(11) Kawano, T.; Niidome, Y.; Mori, T.; Katayama, Y.; Niidome, T. *Bioconjugate Chem.* **2009**, *20*, 209–212.
(12) Lee, H.; Yu, M. K.; Park, S.; Moon, S.; Min, J. J.; Jeong, Y. Y.; Kang, H. W.; Jon, S. *J. Am. Chem. Soc.* **2007**, *129*, 12739–12745.
(13) Wu, Q.; Cao, H.; Luan, Q.; Zhang, J.; Wang, Z.; Warner, J. H.; Watt, A. A. R. *Inorg. Chem.* **2008**, *47*, 5882–5888.
(14) Morales, M. A.; Finotelli, P. V.; Coaquira, J. A. H.; Rocha-Leão, M. H. M.; Diaz-Aguila, C.; Baggio-Saitovitch, E. M.; Rossi, A. M. *Mater. Sci. Eng., C* **2008**, *28*, 253–257.
(15) Murphy, C. J. *J. Mater. Chem.* **2008**, *18*, 2173–2176.
(16) Huang, Q.; Shi, X.; Pinto, R. A.; Petersen, E. J.; Weber, W. J., Jr. *Environ. Sci. Technol.* **2008**, *42*, 8884–8889.
(17) Filip, J.; Zboril, R.; Schneeweiss, O.; Zeman, J.; Cernik, M.; Kvapil, P.; Otyepka, M. *Environ. Sci. Technol.* **2007**, *41*, 4367–4374.
(18) Corbett, J. F. *Dyes Pigm.* **1999**, *41*, 127–136.
(19) Rode, C. V.; Vaidya, M. J.; Chaudhari, R. V. *Org. Process Res. Dev.* **1999**, *3*, 465–470.
(20) Crossley, M. L. *Ind. Eng. Chem.* **1922**, *14*, 802–804.

limitations. Metal oxides in huge amounts are produced as sludge out of these reactions. Therefore, there is a need for an alternative effective and eco-friendly method for nitrophenol reduction. As a consequence, hydrogenation of 4-NP in the presence of various heterogeneous metal catalysts such as Pd,[21] Ni,[22,23] Re,[24] Pt,[25] and TiO_2-supported Ni[26] and reduction of 4-NP by hydrazine in the presence of Raney nickel as catalyst in ethanol−water[27] have been studied. Nitrophenol reduction by borohydride in the presence of suitable catalysts has also been accepted as an alternative route. In this respect, catalytic applications of nanosized Ni,[28] Au and Ag,[29−32] bimetallic Pt−Ni,[33] resin bound silver,[34] and so on could be worth mentioning. A couple of reports are also available, where Cu/Co molybdate and chromium phosphate[35] have been applied as catalysts. Metal oxides of 3d metal ions having spinel type structure with the general formula AB_2O_4 were also used for conversion of 4-NP to 4-AP. As an example, spinel oxide $NiCo_2O_4$[36] showed its efficiency in the reduction of 4-NP. In addition, metal nanoparticles synthesized on polymeric matrix such as poly(acrylic acid)[37] and poly(*N*-isopropylacrylamide)[38] have also shown their worth for catalytic reduction of 4-NP.

Supramolecular architectures of natural carbohydrates have recently attracted much attention as "smart materials" from bio- and nanoengineering perspectives. Polysaccharide hydrogels are suitable as a matrix for cell culture and biomedical applications (viz., tissue engineering, controlled release of drugs enzymes, cell encapsulation,[39,40] etc.) and as a support for enzyme and metal catalysts.[41] These hydrogels contain various functionalities and are stable in most organic solvents. This typical property makes them suitable for catalytic applications.

Alginic acid, which forms the main constituent of brown algae, is a well-known biopolymer and belongs to a polysaccharide family. It is composed of homopolymeric blocks of 1−4-linked β-D-mannuronic acid (M) and α-L-guluronic acid (G). Two acid units M and G are connected with regions of alternating structure in varying proportions of GG, MG, and MM blocks. Hydrosol of sodium alginate is known as a stabilizer and template for synthesis of metal nanoparticles.[42,43] Alginate has mild reducing ability and biocompatibility. It is a renewable bioresource and a low-cost material. This made it ideal for "Green Chemistry" approaches. Alginate gels recently created great interest in the field of medical and biological sciences for tissue engineering due to their nontoxicity and biodegrability.[44,45] It is being used as thickener in food materials and as capsules for drugs. Carboxylic acid groups play an important role of ionic interaction with divalent ions. Aqueous sodium alginate is easily transformed into a hydrogel in the presence of multivalent ions such as Fe^{2+}, Ca^{2+}, Ba^{2+}, Zn^{2+}, and so on with the exception of Mg^{2+}[46] to form an egg-box-like structure. Thus, it can be used as a scaffold for metal nanoparticle impregnation, having the potential for forming a "smart" material. There are not many reports on alginate-stabilized nanoparticles. A few reports include noble metal nanoparticles, namely, Au[42] and Au−Ag[43] prepared in aqueous sodium alginate, and nanoparticles such as Au and Ag,[47] and Co and Ni[48,49] synthesized in calcium alginate gel. In addition to this, alginate was used for magnetic iron oxide nanoparticle preparation.[10] Basically, two strategies prevail: In the first method, metal is incorporated through gelation; that is, the concerned metal ion is used in place of Ca^{2+} for inducing gelation. In the second method, after the gelation is complete, the metal ions are incorporated in the gel through diffusion. In any case, a reduction step is the next prerequisite. Very recently, it was shown that incorporation of already prepared gold nanorods is also possible.[50] Our current aim is to synthesize alginate-supported Ag and Au nanocomposite materials using a greener approach, and to explore its possibility as an eco-friendly heterogeneous catalyst for the conversion of 4-NP to 4-AP using $NaBH_4$ as reducing agent. Heterogeneous reactions present a challenge to several branches of science, namely, chemical kinetics, surface and solid-state physics, and surface chemistry. Besides their fundamental importance to science, heterogeneous reactions play a significant role in many important applications in both the electronic and chemical industries. Thus, research in surface reactivity is an existing forefront in science. The new alginate-stabilized solid-phase silver and gold nanoparticles may thus have much potential to be explored in various catalysis applications. Moreover, heterogeneous systems have great practical advantages over homogeneous ones, notably because of the ease of their separation from the reactants and the products, making the catalyst reusable. To the best of our knowledge, this is the first report of catalytic application of alginate-based nanoparticles for nitrophenol reduction.

Experimental Section

Reagents. All reagents were of analytical grade. Sodium alginate and 4-NP were obtained from LOBA chemicals, India. Calcium chloride, silver nitrate, sodium borohydride, and absolute ethanol were purchased from SRL India. Gold chloride ($HAuCl_4$) was obtained from Aldrich. 4-NP was crystallized

(21) Lakshmi Kantam, M.; Chakravarti, R.; Pal, U.; Sreedhar, B.; Bhargava, S. *Adv. Synth. Catal.* **2008**, *350*, 822–827.
(22) Sugimori, A *Bull. Chem. Soc. Jpn.* **1961**, *34*, 407–411.
(23) Rizhi, C.; Yan, D.; Weihong, X.; Nanping, X. *Chin. J. Chem. Eng.* **2007**, *15*, 884–888.
(24) Belousov, V. M.; Palchevskaya, T. A.; Bogutskaya, L. V.; Zyuzya, L. A. *J. Mol. Catal.* **1990**, *60*, 165–172.
(25) Vaidya, M. J.; Kulkarni, S. M.; Chaudhari, R. V. *Org. Process Res. Dev.* **2003**, *7*, 202–208.
(26) Chen, R.; Du, Y.; Xing, W.; Xu, N. *Chin. J. Chem. Eng.* **2006**, *14*, 665–669.
(27) Goswami, N.; Rahman, M. L.; Huque, M. E.; Qaisuddin, M. *Chem. Technol. Biotechnol.* **1984**, *34*, 195–202.
(28) Chen, R.; Wang, Q.; Du, Y.; Xing, W.; Xu, N. *Chem. Eng. J.* **2009**, *145*, 371–376.
(29) Esumi, K.; Isono, R.; Yoshimura, T. *Langmuir* **2004**, *20*, 237–243.
(30) Panigrahi, S.; Basu, S.; Praharaj, S.; Pande, S.; Jana, S.; Pal, A.; Ghosh, S. K.; Pal, T. *J. Phys. Chem. C* **2007**, *111*, 4596–4605.
(31) Pradhan, N.; Pal, A.; Pal, T. *Langmuir* **2001**, *17*, 1800–1802.
(32) Praharaj, S.; Nath, S.; Ghosh, S. K.; Kundu, S.; Pal, T. *Langmuir* **2004**, *20*, 9889–9892.
(33) Ghosh, S. K.; Mandal, M.; Kundu, S.; Nath, S.; Pal, T. *Appl. Catal., A* **2004**, *268*, 61–66.
(34) Jana, S.; Ghosh, S. K.; Nath, S.; Pande, S.; Praharaj, S.; Panigrahi, S.; Basu, S.; Endo, T.; Pal, T. *Appl. Catal., A* **2006**, *313*, 41–48.
(35) Ghorai, T. K.; Dhak, D.; Azizan, A.; Pramanik, P. *Mater. Sci. Eng., B* **2005**, *121*, 216–223.
(36) Swathi, T.; Buvaneswari, G. *Mater. Lett.* **2008**, *62*, 3900–3902.
(37) Lu, Y.; Mei, Y.; Schrinner, M.; Ballauff, M.; Moller, M. W.; Breu, J. *J. Phys. Chem. C* **2007**, *111*, 7676–7681.
(38) Lu, Y.; Mei, Y.; Ballauff, M. *J. Phys. Chem. B* **2006**, *110*, 3930–3937.
(39) Jiang, Y.; Zhang, L.; Yang, D.; Li, L.; Zhang, Y.; Li, J.; Jiang, Z. *Ind. Eng. Chem. Res.* **2008**, *47*, 2495–2501.
(40) Jiang, Z.; Zhang, Y.; Li, J.; Jiang, W.; Yang, D.; Wu, H. *Ind. Eng. Chem. Res.* **2007**, *46*, 1883–1890.
(41) Guibal, E. *Prog. Polym. Sci.* **2005**, *30*, 71–109.
(42) Pal, A.; Esumi, K.; Pal, T. *J. Colloid Interface Sci.* **2005**, *288*, 396–401.
(43) Pal, A.; Esumi, K. *J. Nanosci. Nanotechnol.* **2007**, *7*, 2110–2115.
(44) Rowley, J. A.; Madlambayan, G.; Mooney, D. J. *Biomaterials* **1999**, *20*, 45–53.
(45) Kuo, C. K.; Ma, P. X. *Biomaterials* **2001**, *22*, 511–521.
(46) Quignard, F.; Valentin, R.; Di Renzo, F. *New J. Chem.* **2008**, *32*, 1300–1310.
(47) Torres, E.; Mata, Y. N.; Blázquez, M. L.; Muñoz, J. A.; González, F.; Ballester, A. *Langmuir* **2005**, *21*, 7951–7958.
(48) Brayner, R.; Vaulay, M. J.; Fiévet, F.; Coradin, T. *Chem. Mater.* **2007**, *19*, 1190–1198.
(49) Brayner, R.; Coradin, T.; Fiévet-Vincent, F.; Livageb, J.; Fiévet, F. *New J. Chem.* **2005**, *29*, 681–685.
(50) Mitamura, K.; Imae, T.; Saito, N.; Takai, O. *J. Phys. Chem. C* **2008**, *112*, 416–422.

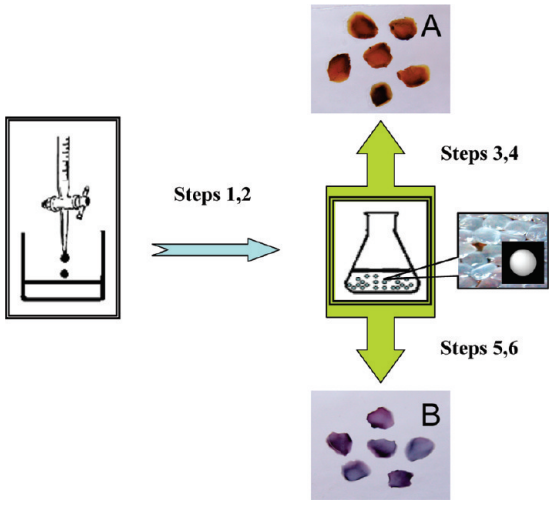

Figure 1. Schematic for the preparation of (A) Ag/CA and (B) Au/CA catalysts. Step 1: Formation of CA beads by dropwise addition of aqueous solution of Na-alginate into $CaCl_2$ solution. Step 2: After cross-linking and thorough washing, the beads were stored in Milli Q water. Steps 3 and 5: Beads were incubated in $AgNO_3$ and $HAuCl_4$ solution, respectively, and UV irradiated. Steps 4 and 6: Ag and Au embedded beads were washed and air-dried in the absence of light.

from alcohol before use. All other chemicals were used as received.

Preparation of Calcium Alginate (CA) Beads. Calcium alginate (CA) beads were prepared by drop by drop addition of aqueous 100 mL solution of Na-alginate (0.4%) (w/v) from a buret to 150 mL of 0.1 M solution of $CaCl_2$ under continual magnetic stirring, keeping the dropping nozzle 1 cm above the $CaCl_2$ solution interface. Presence of divalent Ca^{2+} ions causes gelation to form beads of spherical nature having the diameter of ~2 mm. Freshly formed beads were kept immersed in $CaCl_2$ solution for 24 h for diffusion of more Ca^{2+} ions inside the beads. At this point, it is important to mention that the protonation step as referred to in our earlier work[8] was avoided in the procedure for the efficient catalytic application of the beads. Beads were filtered and washed with Milli Q water several times until the washing was Cl^- free. Finally, these CA beads were stored in Milli Q water for further use. A schematic is shown in Figure 1 (steps 1, 2).

Preparation of Ag Embedded Calcium Alginate (Ag/CA) and Au Embedded Calcium Alginate (Au/CA) Beads using Photochemical Approach. The beads embedded with Ag and Au nanoparticles were prepared using a photochemical approach. To embed the hydrogel beads with Ag nanoparticles, the following procedure was adopted: First, the CA gel beads were taken out of the water. Approximately 3.7 g of beads (containing ~95% water) was incubated with 1 mL of 1.0 mM $AgNO_3$ solution for 3 h and then irradiated using a UV light source (365 nm wavelength) for 40 min with a gap of 10 min between each 10 min of irradiation. After the irradiation, the beads were thoroughly washed and dried for 24 h in air under dark condition. Dried beads were shaped like circular flakes. This is designated as Ag/CA hereafter. The color of the beads was deep yellow (as shown in Figure 1). In a similar approach, Au embedded calcium alginate (Au/CA) beads were prepared using 1.0 mM $HAuCl_4$ in place of $AgNO_3$. The colors of the beads in this case were blue-violet (as shown in Figure 1). The schematic is shown in Figure 1 (steps 3−6).

Reduction of 4-NP Using $NaBH_4$ in the Presence of Dried Ag/CA and Au/CA Beads. The catalytic 4-NP reduction was carried out in a well-stoppered quartz cuvette in the presence of Ag/CA or Au/CA beads and aqueous borohydride. While studying the effect of catalyst dose, the catalyst dose was varied in the range of 0.4−2.0 g/L, keeping the final concentration of 4-NP at 1.0×10^{-4} M and $NaBH_4$ at 0.1 M. To a solution of 2.5 mL of 0.1 M $NaBH_4$, an aliquot of 25 μL of 4-NP stock solution (1×10^{-2} M) was added. At this stage, the nitrophenol was converted to nitrophenolate anion. After that, the catalyst was added. The reaction was spectrophometrically monitored at 400 nm at different time intervals. In a similar way, the study was carried out at various initial concentrations of 4-NP (final concentration in the range $0.6-1.4 \times 10^{-4}$ M) keeping the catalyst dose at 1.2 g/L and borohydride concentration at 0.1 M. The effect of borohydride concentration was studied in the range of ~0.02−0.1 M, keeping the initial 4-NP concentration at 1×10^{-4} M and catalyst dose at 1.2 g/L. The continuous H_2 generation of BH_4^- kept the solution mixing throughout the time of reaction.

Instruments. Absorption spectra were recorded in a Spectrascan UV 2600 spectrophotometer (Chemito, India) equipped with a 1 cm well-stoppered quartz cuvette. Fourier transform infrared (FTIR) spectra were collected in transmittance mode with a Perkin-Elmer Spectrum 1 RX1 FTIR instrument. Dried CA, Ag/CA, and Au/CA beads were cryo-ground and dried, and then the IR spectra were recorded in KBr. High resolution transmission electron microscopy (HRTEM) images were recorded in a ZEOL ZEM 2010 TEM instrument with an accelerating voltage of 200 kV. The aqueous suspension of the cryo-ground sample was prepared and spotted on a Cu grid. Selected area diffraction (SAED) patterns were obtained in the TEM instrument. The EDAX was an Oxford Instruments INCA energy system connected with the TEM. Scanning electron microscopy (SEM) images were accumulated by placing the samples (as-is and not cryo-ground) on a carbon tape in a JEOL JSM 7000F field emission scanning electron microscope. The atomic percentage was determined from EDS data. EDS was carried out with the JEOL JSM 7000F SEM instrument using an OXFORD EDAX system. X-ray diffraction (XRD) analysis was done using powdered samples in atmospheric air in a RINT 2500 X-ray diffractometer (RIGAKU) (operating at 50 kV and 100 mA) using Cu ($K\alpha$ = 1.54056) as the X-ray source. JCPDS software was used for analyzing the crystal planes. Dried beads were cryo-ground and again dried before XRD analysis. Photoirradiation was carried out using a UV light (15 W; Philips, Holland) irradiating at ~365 nm wavelength.

Results and Discussion

Photochemical Reduction of Ag(I) and Au(III) on CA Hydrogel and Formation of Ag/CA and Au/CA Beads. Carbohydrate-based biopolymers such as methyl cellulose,[51] starch,[52] cellulose fibers,[53] chitosan,[54] and so on which are nontoxic in nature are currently being used as a support for nanoparticles for their possible applications in biomedical research. Carbohydrate-based synthetic polymers are also in use for nanoparticle synthesis.[29,55] Both chemical[56] and photochemical[57,58] approaches are available for the reduction of metal ions onto these polymers. The functionalities present in those polymers have the advantage of being photochemically active and, at the same time, supportive for nanoparticles stabilization. While the chemical approach requires an excess of chemicals such as sodium borohydride, hydrazine, formic acid, and so on, leading to unwanted toxicity, and environmental as well as biological risk,

(51) Pal, A.; Stokes, D. L.; Vo-Dinh, T. *Curr. Sci.* **2004**, *87*, 486–491.
(52) Raveendran, P.; Fu, J.; Wallen, S. L. *J. Am. Chem. Soc.* **2003**, *125*, 13940–13941.
(53) He, J.; Kunitake, T.; Nakao, A. *Chem. Mater.* **2003**, *15*, 4401–4406.
(54) Murugadoss, A.; Chattopadhyay, A. *Nanotechnology* **2008**, *19*, 015603–015611.
(55) Zhao, M.; Sun, L.; Crooks, R. M. *J. Am. Chem. Soc.* **1998**, *120*, 4877–4878.
(56) Morones, J. R.; Frey, W. *Langmuir* **2007**, *23*, 8180–8186.
(57) Esumi, K.; Matsuhisa, K.; Torigoe, K. *Langmuir* **1995**, *11*, 3285–3287.
(58) Esumi, K.; Suzuki, A.; Aihara, N.; Usui, K.; Torigoe, K. *Langmuir* **1998**, *14*, 3157–3159.

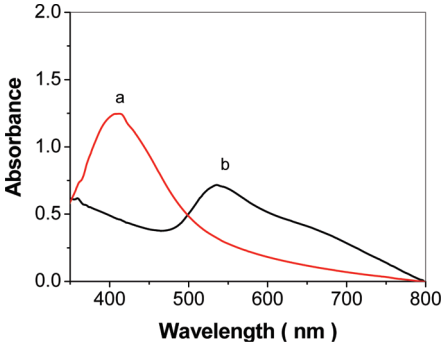

Figure 2. UV−vis absorption spectra of Ag-embedded (curve a) and Au-embedded (curve b) CA hydrogel beads.

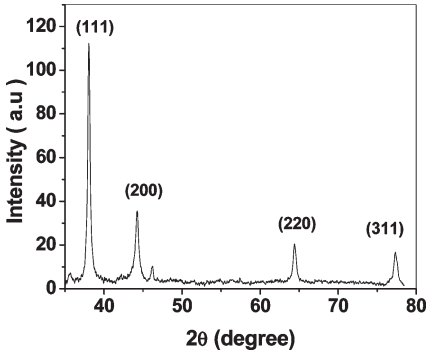

Figure 3. XRD of cryo-ground Ag/CA beads.

photochemical approaches are more attractive because of the simplicity and their less hazardous pathways. In our present study, a convenient and "green" photochemical procedure was put forward for the reduction of Ag(I) and Au(III) onto CA hydrogel beads. Sodium and calcium alginate have a large abundance of carboxylate and hydroxyl functionalities, which helps them to act as both a reductant and a stabilizer.[42,43] Earlier literature documents[47] that Ag(I) and Au(III) ions can lead to aggregated Ag and Au nanoparticles if kept in contact with alginate for long periods of time. In the current approach, the UV activation technique helps such a reduction to occur within a short time period (40 min) to lead to Ag embedded CA (Ag/CA) beads and Au embedded CA (Au/CA) beads.

The sorption of Ag(I) and Au(III) by CA hydrogel beads will depend on the solution pH. Also, during the sorption, the solution pH may change due to proton exchange. In our experiment, during the sorption of $AgNO_3$ onto the gel beads, the pH was ∼6 and no pH change was noticed throughout the adsorption process. On the other hand, the pH was ∼2 at the start of $HAuCl_4$ sorption. Gradually, the solution pH was increased during the sorption and finally reached ∼6. This is due to the proton exchange. This phenomenon was reported by Torres et al.,[47] where it was also mentioned that sorption of $HAuCl_4$ in CA beads is best at lower pH whereas $AgNO_3$ sorption is favored at higher pH.

The white semitransparent gel beads turned yellow upon 10 min of irradiation with $AgNO_3$ and darkened further on successive irradiations. On the contrary, the hydrogel beads turned blue-violet when irradiated in the presence of $HAuCl_4$. UV−visible spectra of Ag- and Au-embedded CA hydrogel beads show surface plasmon bands at 410 nm (curve a) and 534 nm (curve b), respectively (Figure 2), which readily speaks about the formation of Ag and Au nanoparticles, respectively, in the gel. The uptake of silver and gold from their solutions by alginate varied depending on the concentration of $AgNO_3$ and $HAuCl_4$. It is observed from the EDS analysis that under identical conditions an increase of $AgNO_3$ concentration from 10^{-4} to 10^{-3} M could increase the Ag deposition from 0.66 to 16.56 atom % (∼25 times). Similarly, an increase of $HAuCl_4$ concentration from 0.5×10^{-3} to 10^{-3} M could increase the Au deposition from 0.09 to 0.33 atom % (∼4 times). However, for better catalytic efficiency with the same dose of catalyst, Ag/CA and Au/CA with higher loading were selected. The dried beads remain stable for several months under ambient conditions. To avoid any unwanted efficiency loss, however, they were stored in stoppered amber-colored bottles.

The percentage of silver and gold ions adsorbed onto the CA beads and finally reduced to zero state was estimated by spectrophotometric method. The calibration curves generated at 220 nm for $AgNO_3$ and 290 nm for $HAuCl_4$ (with correlation coefficient ∼ 0.99) were used to quantify the amount of Ag^+ and $AuCl_4^-$ remaining in the solution phase after the photoreduction and thorough wash. It was observed that ∼30% loading in the case of silver and ∼90% loading in the case of gold took place on the CA hydrogel beads. This led to a loading of 175 μg of Ag per gram of dry Ag/CA and 958 μg of Au per gram of dry Au/CA. To understand whether the photoreduction of the metal ions in the gel was complete, an indirect experiment was performed. After the photoreduction and thorough wash, the beads were dissolved in ∼0.1 M NaOH and the UV−visible absorption spectra were recorded. The solution on dissolution of Ag/CA hydrogel beads looked light yellow, and the characteristic band appeared at 406 nm. On the other hand, the solution after the dissolution of Au/CA hydrogel beads looked blue-violet and the band appeared at 532 nm. This clearly revealed the existence of Ag(0) and Au(0) in the respective solutions. On subsequent addition of $NaBH_4$ to the resultant solutions, no change in the absorbance values at the corresponding absorption maxima of Ag(0) and Au(0) was noticed. This revealed that after photoreduction there was no residual silver or gold ions left on the Ag/CA and Au/CA beads, indicating that the photoreduction was complete.

Fourier Transform Infrared Study. It is important to know how the participation of alginate occurs as a reductant. This can be clearly understood from the FTIR spectra of dried CA, Ag/CA, and Au/CA beads. In our earlier work,[8] it was shown that the secondary hydroxyl group present in the polysaccharide moiety brings about the reduction of Ag(I) and Au(III) with the concomitant photooxidation of >CHOH leading to the formation of a new >C═O functionality. This type of phenomenon, that is, reduction of metal ions, such as Au(III) to Au (0), and oxidation of >CHOH to >C═O, has been observed before in cases of sugar persubstituted poly(amidoamine) dendrimers,[59] catechol,[60] Triton X-100,[61] and so on using photoactivation techniques. The FTIR spectra of dried beads of CA (curve a), Ag/CA (curve b), and Au/CA (curve c) are shown in Supporting Information Figure S1. In the present study, the FTIR spectra of Ag/CA or Au/CA did not show distinct peaks at ∼1730 cm^{-1} (as was clearly observed in our previous case[8]). In the FTIR spectra of CA, Ag/CA, and Au/CA, the peaks appearing at ∼1420 and ∼1609 cm^{-1} are due to the symmetric and antisymmetric stretching vibrations of $-COO^-$, respectively.[8,47] The broad bands in the range of 3408 cm^{-1} for CA, Ag/CA, and Au/CA indicates the presence of −OH groups in all cases.

X-ray Diffraction Study for Particle Characterization. The XRD spectrum of Ag/CA shown in Figure 3 confirms the

(59) Esumi, K.; Hosoya, T.; Suzuki, A.; Torigoe, K. *J. Colloid Interface Sci.* **2000**, *226*, 346–352.
(60) Pal, A. *Mater. Lett.* **2004**, *58*, 529–534.
(61) Pal, A. *Talanta* **1998**, *46*, 583–587.

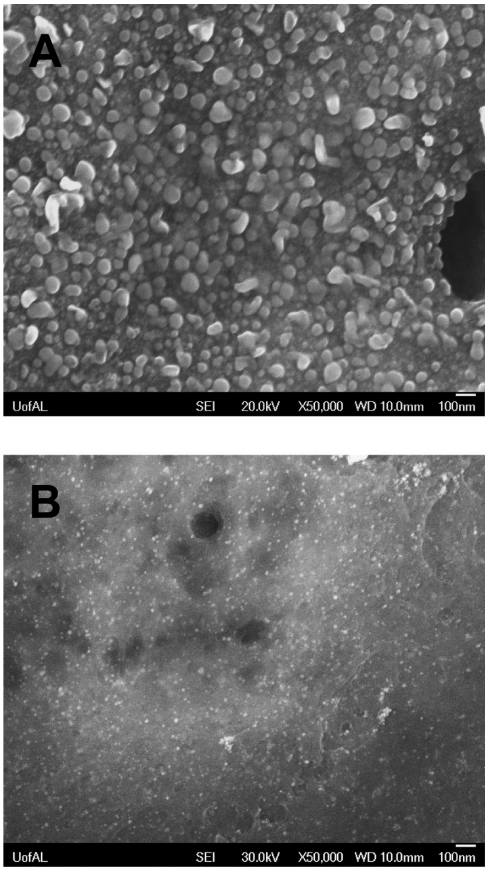

Figure 4. SEM images of dried (A) Ag/CA and (B) Au/CA.

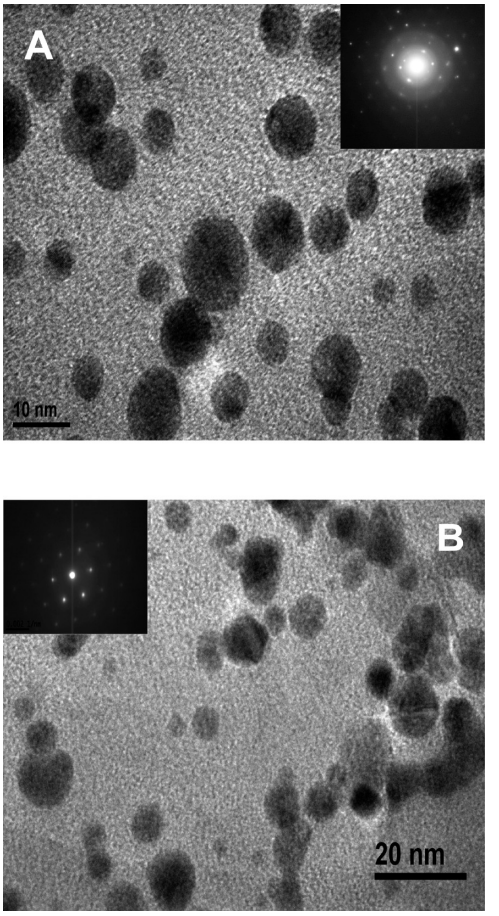

Figure 5. TEM images of cryo-ground beads of (A) Ag/CA and (B) Au/CA. SAED patterns are shown in the insets.

formation of single crystalline Ag nanoparticles in Ag/CA. Bragg's reflections at 2θ = 38.2°, 44.3°, 64.5°, and 77.4° correspond to {111}, {200}, {220}, and {311} lattice planes, respectively, for the face-centered cubic (fcc) structure of silver nanoparticles embedded in CA. The XRD pattern also shows that the size of the particles is in the nanometer range.[62] No diffraction peaks corresponding to silver oxide are observed. It is known that Au and Ag crystals have similar lattice parameters (0.408 and 0.409 nm, respectively), which results in the similarity in their XRD patterns.[8] In the present case, Au/CA also shows similar XRD patterns, but with less intensity than that of Ag/CA, indicating similar lattice planes.

Scanning and Transmission Electron Microscopic Studies. Scanning electron microscopy (SEM) studies on Ag/CA and Au/CA dried beads were performed to gain information about the particle morphologies. The Ag particles embedded on Ag/CA are mostly spherical and closely packed (Figure 4A). As observed from the SEM image of Ag/CA, silver particles fully cover the alginate surface. On the other hand, the coverage of the alginate surface by Au particles on Au/CA is much less (Figure 4B). The Au nanoparticles are embedded in the matrix in a scattered manner, and the particles are spherical in nature. Energy dispersive spectroscopy (EDS) of Ag/CA and Au/CA shows that the atomic percentages of Ag and Au in Ag/CA and Au/CA were 16.56% and 0.33%, respectively. In the sorption experiment, although the sorption of Au was found to be more compared to that of Ag, the atomic percentage of Ag in Ag/CA, as observed in EDS, is more compared to that of Au in Au/CA. This observation may be because silver ions were more concentrated on the surface of the CA beads, whereas the gold ions were more diffused inside the CA beads.

Transmission electron microscopy (TEM) analysis provides information about the size and shape of the Ag and Au nanoparticles supported on CA matrix. The particles are spherical, and the size ranged within 7 ± 2 nm for Ag particles (Figure 5A) and 5 ± 2 nm for Au particles (Figure 5B). The SAED patterns of Ag and Au nanoparticles are shown in the insets of Figure 5A and B, respectively, which clearly indicate their crystalline nature.

One important observation regarding the size range observed for Ag particles in SEM and TEM is that in SEM they look much bigger. The reason behind this may be the sampling procedure. In the case of SEM, the analysis was done by placing the sample as such on a carbon tape. However, for TEM, the samples were prepared by cryo-grinding the sample followed by making a suspension and then sonication. After that, the sample was placed on a copper grid and the TEM image was taken. Thus, in SEM images, we see the larger particles having a substructure with smaller particles held together by relatively weak forces. These smaller particles presumably fall apart during the cryo-grinding and sonication, which we see in the TEM image. In the case of Au/CA, however, the particle size looks consistent in SEM and TEM images.

Catalytic Reduction of 4-Nitrophenol. The catalytic activity of as-prepared alginate biopolymer based Ag and Au nanoparticles were substantiated through 4-NP reduction in the presence of borohydride as a reductant. This reaction using noble metal nanoparticles as catalysts[31] recently has become one of the model reactions for evaluating the catalytic activity of various metal

(62) Zhu, J.; Kónya, Z.; Puntes, V. F.; Kiricsi, I.; Miao, C. X.; Ager, J. W.; Alivisatos, A. P.; Somorjai, G. A. *Langmuir* **2003**, *19*, 4396–4401.

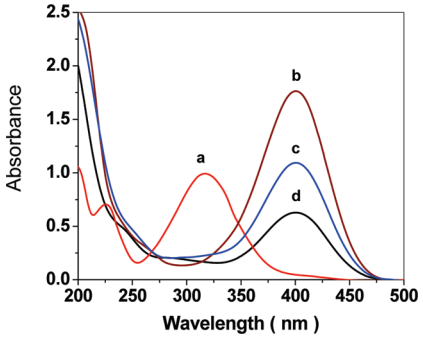

Figure 6. Adsorption of 4-NP on dried CA beads. Absorption spectra of 4-NP (a) In absence of $NaBH_4$, (b)-(d) In presence of $NaBH_4$ at 0 min, 1 and 16 h, respectively. Conditions: [4-NP] = 1.0×10^{-4} M; [CA] = 1.2 g/L; [$NaBH_4$] = 0.1M.

nanoparticles such as Ag, Au, Cu, Pt, and Pd in different substrates such as dendrimers, polyelectrolytes, biological cells, and so on.[63−65] Although the reaction is a thermodynamically feasible process involving E_0 for 4-NP/4-AP = −0.76 V and H_3BO_3/BH_4^- = −1.33 V versus NHE, it is kinetically restricted (does not occur even in 2 days' time) in the absence of a catalyst. Under alkaline conditions, the decomposition of borohydride is much slower. Borohydride is relatively environmentally friendly because of the low toxicity of borates. The advantage of the catalytic reduction of 4-NP is the easy monitoring of the reactant 4-nitrophenolate anion (λ_{max} = 400 nm) through spectrophotometry. The 4-nitrophenolate anion formation from 4-NP (pK_a = 7.15) in the initial step upon addition of borohydride is indicated when the peak at 317 nm (due to 4-NP) is shifted to 400 nm. The sole product 4-AP (λ_{max} = 293 nm) can also be monitored easily, and when required to know whether the reduction is actually taking place. Under certain situations, a significant decrease in absorbance at 400 nm may not be associated with the concomitant evolution of a peak at 293 nm indicating that the process does not involve any reduction, rather it is a mere adsorption of the nitrophenolate ion.[65] This is a very important step that must be critically observed. In our case, because CA is a known bioadsorbent[47,66] with a porous structure, there is the possibility of adsorption of the parent reactant on the heterogeneous surface of CA. To understand this phenomenon, the reaction was carried out under similar reaction conditions using dried CA beads (i.e., the base material without nanoparticles), and the time dependent absorption spectra were obtained (Figure 6). The figure shows that the red shift of the absorption maximum of 4-NP at 317 nm (Figure 6, curve a) to 400 nm (Figure 6, curve b) takes place on addition of borohydride due to nitrophenolate ion formation. On further keeping the solution for a longer time, a significant decrease in the intensity of the peak at 400 nm (characteristic band for 4-nitrophenolate ion) is observed at 1 h (curve c) and 16 h (curve d). It is also clear from the figure that in this case the decrease in absorbance is due to adsorption of 4-nitrophenolate on CA but not due to reduction, because there is no new peak at 293 nm. This also validates the importance of metal nanoparticles for the reduction process. This has a resemblance with the earlier observation by Sharma et al.[65]

On the other hand, the catalytic activity of Ag/CA and Au/CA toward 4-NP reduction is convincingly demonstrated by the

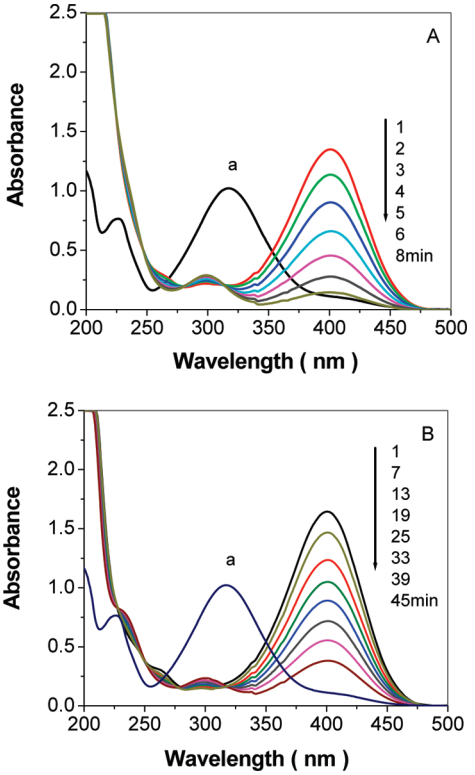

Figure 7. Time dependent absorption spectra for the catalytic reduction of 4-NP by $NaBH_4$ in presence of (A) Ag/CA, and (B) Au/CA. Conditions: [4-NP] = 1.0×10^{-4}M; [Catalyst] = 1.2 g/L; [$NaBH_4$] = 0.1M.

spectrophotometric studies (Figure 7A and B, respectively). Curve a in both panels depicts the absorption spectrum of 4-NP in the absence of $NaBH_4$. The shift of the peak at 400 nm on addition of $NaBH_4$ and its successive decrease with time indicates the catalytic reduction of 4-NP to 4-AP. The catalytic reduction was much faster in the case of Ag/CA compared to Au/CA. The isosbestic points clearly found at 247, 278, and 314 nm in the case of Ag/CA and at 228, 250, 279, and 316 nm in the case of Au/CA show that 4-AP is the sole product of the reaction.[67] It is also important to note here that the reduction started immediately after the addition of the catalyst and there was no induction time required. This is in contrary to the other literature involving Pt, Pd, and Ag composite.[64,67−69] The induction time usually relates to the presence of dissolved oxygen in water reacting at a faster rate with borohydride than nitrophenol. To avoid this, in many cases, nitrogen is purged before adding $NaBH_4$. In our case, however, such a technique is not involved, and the catalytic reaction was carried out under atmospheric conditions. This might be advantageous in terms of easiness for real technological applications. Moreover, the liberated hydrogen from borohydride purged out the air, and this condition prevents the aerial oxidation of 4-AP. In addition, evolution of small bubbles on the catalyst surface helped in stirring/well mixing the solution. As a result, catalyst particles remain distributed in the reaction mixture during the reaction time, offering favorable conditions for a smooth reaction to occur.

The efficiency of a reaction may further be judged from the yield of the product. The percentage yield of 4-AP at the end of the

(63) Hayakawa, K.; Yoshimura, T.; Esumi, K. *Langmuir* **2003**, *19*, 5517–5521.
(64) Mei, Y.; Sharma, G.; Lu, Y.; Ballauff, M.; Drechsler, M.; Irrgang, T.; Kempe, R. *Langmuir* **2005**, *21*, 12229–12234.
(65) Sharma, N. C.; Sahi, S. V.; Nath, S.; Parsons, J. G.; Gardea- Torresde, J. L.; Pal, T. *Environ. Sci. Technol.* **2007**, *41*, 5137–5142.
(66) Chen, J. P.; Hong, L.; Wu, S.; Wang, L. *Langmuir* **2002**, *18*, 9413–9421.
(67) Mei, Y.; Lu, Y.; Polzer, F.; Ballauff, M. *Chem. Mater.* **2007**, *19*, 1062–1069.
(68) Lu, Y.; Mei, Y.; Drechsler, M.; Ballauff, M. *Angew. Chem.* **2006**, *45*, 813–816.
(69) Pradhan, N.; Pal, A.; Pal, T. *Colloids Surf., A* **2002**, *196*, 247–257.

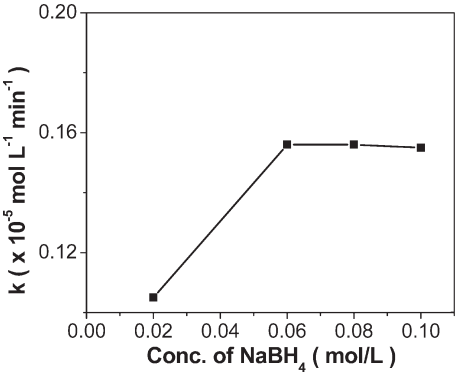

Figure 8. Effect of $NaBH_4$ concentration on catalytic reduction of 4-NP in the presence of Au/CA. Conditions: [4-NP] = 1.0×10^{-4} M; [Au/CA] = 1.2 g/L.

reaction was estimated spectrophotometrically. The calibration curve was generated at λ_{max} = 293 nm (the characteristic band of 4-AP under the experimental conditions applied). It was noticed that under the conditions applied ([catalyst] = 1.2 g/L, [4-NP] = 1×10^{-4} M, [BH_4^-] = 0.1 M), at 8 min time of reaction using Ag/CA, the yield of 4-AP was ~99% and at 50 min time using Au/CA as the catalyst the yield of 4-AP was ~92%. Also, the kinetic analysis performed on the increase of the peak at 293 nm was performed. This showed zero-order kinetics (correlation coefficient ~ 0.97) with respect to 4-AP concentration, and can be correlated with 4-NP consumption. In the time scale, the 4-nitrophenolate reduction is much faster than the adsorption. Thus, decrease of the peak at 400 nm reflects mostly the catalytic reduction of 4-NP to 4-AP.

It is also important to mention at this point that because alginate is a natural functionalized material, the possibility of borohydride to react with the base material CA may not be ruled out. To investigate whether the functionality in the base material of Ag/CA or Au/CA changes after 4-NP reduction using borohydride, FTIR studies were performed on the Ag/CA catalyst after its use. The FTIR spectrum of the used Ag/CA beads when compared with that of CA looks similar, and no new peaks appeared. This indicates that $NaBH_4$ does not react with alginate under the present experimental condition.

The effect of $NaBH_4$ concentration on the reduction rate was studied to select the concentration of $NaBH_4$. As depicted in Figure 8, in the case of 4-NP reduction using Au/CA as catalyst, it was found that in the concentration range 0.02−0.06 M of borohydride the rate increased with the increase in BH_4^- concentration, and in the range of 0.06−0.1 M it remained constant. Thus, the borohydride concentration selected for our entire study was 0.1 M, which is a large excess compared to that of 4-NP, to make the reaction independent (zero-order) of borohydride concentrtion. The kinetics of 4-NP reduction in the presence of Ag/CA and Au/CA catalyst has been studied by monitoring the absorbance at 400 nm due to 4-nitrophenolate anion under varying catalyst doses (0.4−1.6 g/L for Ag/CA and 0.8−2.0 g/L for Au/CA) and under varying initial 4-NP concentrations ($0.6-1.4 \times 10^{-4}$ M). The reaction was much faster when Ag/CA was the catalyst as compared to Au/CA. The various possible reasons may be either the better catalytic efficiency of Ag nanoparticles compared to that of Au nanoparticles or may be either the amount of loading of the metal or the surface coverage. It is estimated from the sorption experiment that loading in the case of Au is much more compared to Ag. Also it is clear from the SEM image that in Ag/CA the surface is almost fully covered with Ag. In the case of Au/CA, the surface coverage is much less. Very

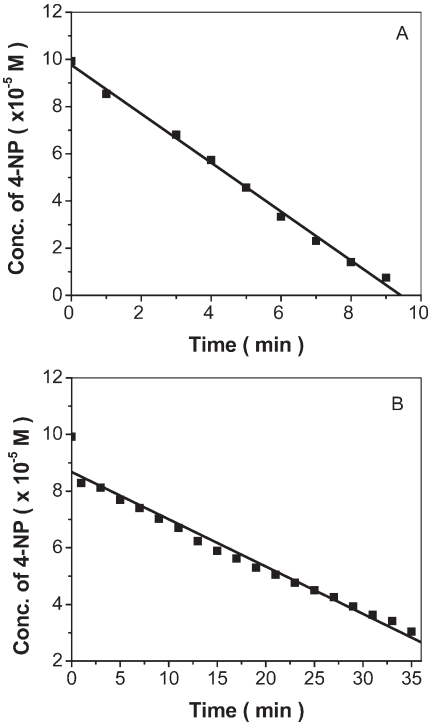

Figure 9. Concentration versus time plot for 4-NP reduction using (A) Ag/CA and (B) Au/CA as catalyst. Conditions: [4-NP] = 1.0×10^{-4} M; [catalyst] = 1.2 g/L; [$NaBH_4$] = 0.1 M.

recently, surface coverage has been demonstrated to be an important factor for controlling the reaction kinetics/mechanism and product selectivity.[70] In order to investigate the mechanism, zero-order, first-order, and second-order kinetic models were tested, and the kinetics operative for 4-NP reduction was assumed on the basis of best correlation obtained. In earlier reports, 4-NP reduction using metal nanoparticles was shown to be pseudo-first-order in the presence of homogeneous[29,67] or heterogeneous catalyst[30,34] However, in the present case, the reduction follows zero-order kinetics with respect to 4-nitrophenolate ion concentration with both Ag/CA and Au/CA as catalyst (Figure 9A and B, respectively). Although in surface catalysis zero-order reactions are common, this change in reaction order indicates that the reduction occurs via different rate-determining steps. One important observation in the case of Au/CA catalyst is the marked drop in 4-nitrophenolate ion concentration during the initial start of the reaction. This can be attributed to sorption into CA beads due to the gradient difference between the solution phase and the solid beads.[71] This is not clearly identified in the case of Ag/CA because the 4-NP reduction is too fast.

Effect of 4-NP Concentration and Catalyst Dose. The 4-NP reduction was studied with various initial 4-NP concentrations (in the range $0.6-1.4 \times 10^{-4}$ M), and the zero-order reaction rate constants (k) were compared. The rate constants for a zero-order reaction should not depend on the initial concentrations of 4-NP, and this has been reflected in the parallel curves a−c in Figure 10A and B, showing the 4-NP reduction using Ag/CA and Au/CA, respectively. The other parameters such as catalyst dose and borohydride concentration remained the same. The k values for Ag/CA catalyzed reaction considering zero-order kinetics varied in the range $1.03-1.04 \times 10^{-5}$ mol/L/min, whereas for

(70) Zaera, F. *Acc. Chem. Res.* **2002**, *35*, 129–136.
(71) Bezbaruaha, A. N.; Krajangpana, S.; Chisholmb, B. J.; Khana, E.; Bermudeza, J. J. E. *J. Hazard. Mater.* **2009**, *166*, 1339–1343.

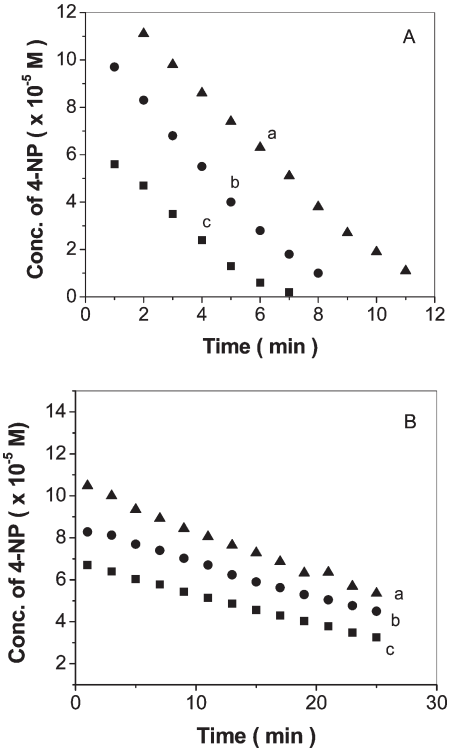

Figure 10. Concentration versus time plot for 4-NP reduction by $NaBH_4$ in the presence of (A) Ag/CA at various initial concentrations of 4-NP (a) 14×10^{-5} M, (b) 12×10^{-5} M, and (c) 8×10^{-5} M and (B) Au/CA at various initial concentrations of 4-NP (a) 12×10^{-5} M, (b) 10×10^{-5} M, and (c) 8×10^{-5} M. Conditions: [catalyst] = 1.2 g/L; [$NaBH_4$] = 0.1 M.

Au/CA as catalyst the k values varied in the range $0.14-0.20 \times 10^{-5}$ mol/L/min. In all cases, the curves showed an excellent correlation coefficient (~0.99). In the case of heterogeneous or microheterogeneous catalysis, the reaction rate generally increases linearly with the amount of catalyst.[30,34,72] The rate constant obtained from the slope of the kinetic curves has been related to catalyst dose, keeping other parameters such as initial 4-NP concentration and borohydride concentration the same. It was observed that with the increased amount of catalyst the rate constant increases in both cases and had a linear relationship. This is obvious because an increase of dose means an increase of surface area. The results for catalytic reduction of 4-NP using Ag/CA are shown in Figure 11.

Temperature Dependence and Activation Energy Calculation. Activation energy (E_a) is an empirical parameter for all chemical reactions, which shows the temperature dependency of the rate constant for a catalysis reaction. The Arrhenius equation shows

$$k = A\, e^{-E_a/RT}$$

where A is a constant known as the Arrhenius factor, k is the rate constant of the reaction at temperature T (in Kelvin), and R is the universal gas constant. The catalytic reduction of 4-NP was studied at three different temperatures 293, 300, and 306 K using Ag/CA and 291, 298, and 306 K using Au/CA as catalysts. The rate constant (k) values were found out under the reaction conditions: [BH_4^-] = 0.1 M, [4-NP] = 1×10^{-4} M, and [catalyst] = 1.2 g/L. A plot of ln k versus $1/T$ shows a linear curve for 4-NP

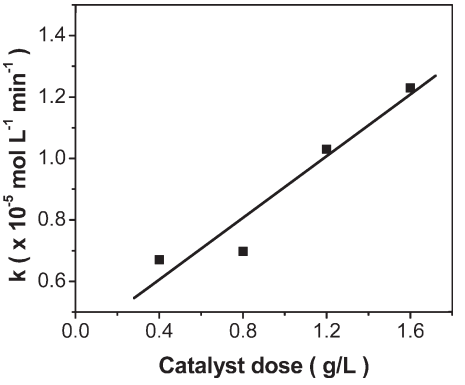

Figure 11. Plot of rate constant (k) versus catalyst dose for 4-NP reduction by $NaBH_4$ in the presence of Ag/CA as catalyst. Conditions: [4-NP] = 1.0×10^{-4} M; [$NaBH_4$] = 0.1 M.

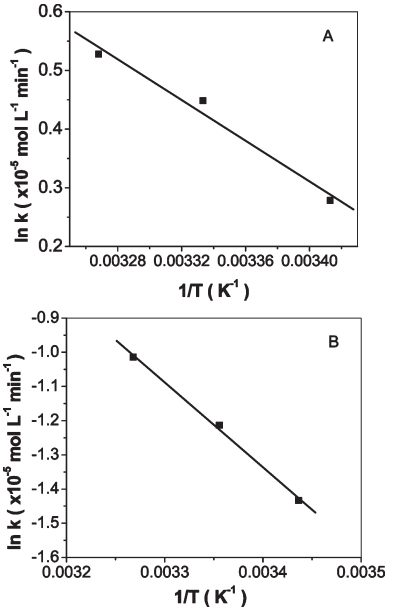

Figure 12. Plot of ln k versus $1/T$ for 4-NP reduction by $NaBH_4$ at different temperatures in the presence of (A) Ag/CA and (B) Au/CA as catalyst. Conditions: [4-NP] = 1.0×10^{-4} M; [catalyst] = 1.2 g/L; [$NaBH_4$] = 0.1 M.

reduction using both Ag/CA and Au/CA catalysts (Figure 12A and B, respectively). It was observed that the value of k increases with the increase in temperature. The activation energy was finally calculated from the slope of the straight line. The activation energy was found to be 3.3 kcal/mol for the Ag/CA catalyzed reaction, and 4.9 kcal/mol for the Au/CA catalyzed reaction. Usually, for surface catalyzed reactions, the activation energy lies within 2−10 kcal/mol. This is a clear indication that the 4-NP reduction in our case occurs via surface catalysis. This can also be supported from the order of the reaction that the reaction is following.

Turnover Frequency (TOF) and Recyclability of the Catalyst. The catalyst turnover number (TON) and the turnover frequency (TOF) are two important quantities used for comparing catalyst efficiency. In heterogeneous catalysis, the TON is the number of reactant molecules that 1 g of catalyst can convert into products.[73] The TOF is simply TON/time. For Ag/CA and Au/CA as the catalysts, using 1.0×10^{-4} M concentration of 4-NP

(72) Jana, S.; Pande, S.; Panigrahi, S.; Praharaj, S.; Basu, S.; Pal, A.; Pal, T. *Langmuir* **2006**, *22*, 7091–7095.

(73) Rothenberg, G. *Catalysis: Concepts and Green Application*; Wiley-VCH Verlag GmbH & Co. KGaA: Weinheim, 2008; p 11.

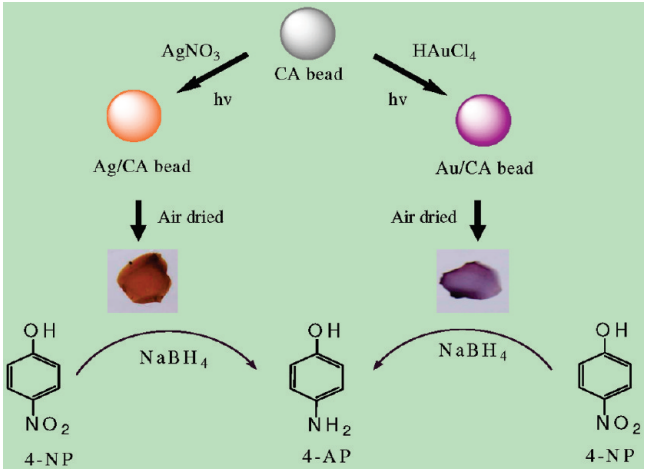

Figure 13. Schematic for the catalytic reduction of 4-NP by $NaBH_4$ in the presence of dried Ag/CA and Au/CA beads.

and 1.2 g/L catalyst dose, the TOF was found to be 9.3×10^{16} and 1.7×10^{16} molecules/g/s, respectively.

A number of reports are available on the catalytic reduction of 4-NP in homogeneous or heterogeneous media. A catalyst supported on solid matrix has always been appreciated in the case of expensive catalysts because of their recyclability. This makes the process cost-effective. In the present, experiment both the catalysts Ag/CA and Au/CA are good in terms of their recyclable property. After completion of one catalytic reduction cycle, a fresh batch of 4-NP was added to the reaction mixture. The availability of a higher concentration of $NaBH_4$ in the reaction mixture easily converted the fresh dose of nitrophenol to nitrophenolate, which is necessary for the reduction to proceed. One interesting feature of the catalyst is that up to third cycle of operation the catalytic efficiency increases and lesser time is required for the 4-NP reduction, and then the efficiency remains almost constant. Such an increase in rate may be because the catalyst becomes more diffusible or may be because the catalyst surface becomes refreshed as the cycle goes on.[74] This is certainly an advantage in terms of the applications and cost-effectiveness of the material. Another interesting observation is that, after the first cycle of operation in the case of Ag/CA catalyst, the 4-NP reduction typically follows the first-order reaction with a very good correlation coefficient (~0.99). This is not the case for the Au/CA catalyst.

Insight on the Catalytic 4-NP Reduction. The catalytic reduction of 4-NP to 4-AP is schematically presented in Figure 13. It is a six-electron transfer process. The role of metal particles in various redox reactions can be explained by electrochemical current potential.[75,76] In the present case, electron transfer takes place from BH_4^- to 4-NP through adsorption of the reactant molecules on to the catalyst surface. The heterogeneous catalysis reaction may occur in four steps: (1) adsorption of the reactant molecule to the surface, (2) diffusion of the molecule to the active site and formation of the surface complex, (3) reaction of the complex to form the adsorbed product, and (4) finally desorption of the product. Among all the steps, the slowest step decides the overall order of the reaction. In our case, both of the catalysts lead to zero-order reactions indicating the possibility that step (3) is the slowest one. The mechanism, in the case of heterogeneous catalysis, depends on many factors, namely, the adsorption behavior of the molecules, the concentration, surface coverage, and the nature of the substrate. For example, if the adsorption tendency is strong, adsorption sites on the surface will be completely covered over a broad range of reactant pressure (P) or concentration (C), and the rate will be independent of P or C as long as the surface is covered. Since the present reaction is a bimolecular reaction, depending on whether one or both molecules are adsorbed on the surface, either of the two models, namely, Langmuir−Hinshelwood or Eley−Rideal, is conceived.[73] To gain further insight into the detailed mechanism, however, more work is warranted.

Conclusion

Biopolymer calcium alginate gel beads were used as a template for silver and gold nanoparticle growth using a green photochemical approach. The alginate served as both a reductant and a stabilizer. The particles were characterized by UV−visible spectroscopy, XRD, SEM, TEM, EDS, and SAED analysis, and they were found to be spherical and crystalline, and with sizes of < 10 nm. The loading of Au was much greater compared to that of Ag on alginate, as estimated from the sorption experiment. The effectiveness of the as-prepared solid-phase alginate-stabilized Ag and Au as catalyst for 4-NP reduction to 4-AP by excess borohydride has been evaluated. The reaction was much faster in the case of Ag/CA compared to that of Au/CA. The reason behind this may be that Ag is a better catalyst or it may be due to the difference in surface coverage. In both cases, the reaction was very efficient and followed zero-order kinetics well. The catalyst efficiency was determined on the basis of TOF and recyclability. The Ag catalyst showed much higher efficiency than the Au catalyst. The new as-prepared biopolymer-based Ag and Au catalysts are stable, efficient, eco-friendly, easy to prepare, and recyclable and thus have potential for industrial applications.

Acknowledgment. The authors are thankful to the reviewers for constructive comments and suggestions. The financial assistance from UGC, New Delhi and IIT, Kharagpur is gratefully acknowledged.

Supporting Information Available: FTIR spectra of dried beads of CA, Ag/CA, and Au/CA. This material is available free of charge via the Internet at http://pubs.acs.org

(74) Pal, T.; Sau, T. K.; Jana, N. R. *Langmuir* **1997**, *13*, 1481–1485.
(75) Miller, D. S.; Bard, A. J.; Mclendon, G.; Ferguson, J. *J. Am. Chem. Soc.* **1981**, *103*, 5336–5341.
(76) Graetzel, M.; Fran, A. J. *J. Phy. Chem. B* **1985**, *89*, 1074–1077.